IR absorption measurements of the velocity of a premixedhydrogen/air flame propagating in a obstacle-laden tube

R. Scarpa, E. Studer, B. Cariteau, S. Kudriakov, N. Chaumeix

IR absorption measurements of the velocity of a premixed hydrogen/air flame propagating in a obstacle-laden tube

Roberta Scarpa, Etienne Studer, Benjamin Cariteau, Sergey Kudriakov,
DEN-STMF, CEA, Université Paris-Saclay,
France

Nabiha Chaumeix,
ICARE,
CNRS Orléans, France

Flame acceleration and explosion of hydrogen/air mixtures remain key problems for severe accident management in nuclear power plants. Empirical criteria have been developed in the early 2000s by Dorofeev and colleagues [1] providing effective tool to discern possible FA or DDT scenarios. A huge experimental database, composed mainly by middle-scale experiments in smooth tubes and obstacle-laden ducts, has been used to validate these criteria. In these devices the position of the reaction front is usually detected by photo-diodes or photomultiplier tubes uniformly distributed along the tube axis. As a result, only a coarse representation of the velocity profile can be achieved.

In this paper we develop a new technique to track the flame position along the tube at any time. This method consists in performing time-resolved IR absorption measurements by doping the fresh mixture with an alkane. The velocity profile is then derived by measuring the variation of the extension in depth of the unburnt gas along the tube axis. Correction factors are eventually drawn from the comparison between longitudinal (IR absorption measurements) and cross-sectional (photomultiplier tubes) flame velocity diagnosis techniques. Finally, experimental results are compared to numerical simulations [2] and analytical models proposed in the literature [3].

Keywords: H2/air mixture, Flame acceleration, Flame speed, Diagnostics for reactive systems, IR absorption, HeNe laser

1 Introduction

In case of severe accident, in-core metal-water reactions due to fuel temperature increase lead to massive release of hydrogen into the containment of Light Water Reactors. The highly compartmentalization of these buildings makes non-condensable gases to accumulate in clouds. With ease, a flammable atmosphere can locally be achieved. Eventually, the explosion of such a cloud may damage those safety features that ensure accident management, jeopardizing the integrity of the containment as well.

The dynamic of combustion reactions is strongly influenced by boundary conditions: confined geometries tend in fact to promote flame acceleration. Under certain circumstances, the overpressure generated by the

lead shock ahead of the flame may cause structural failure. Moreover, since hydrodynamic forces depend on the drag force as well as on the acceleration of the flow field [4], structural damage becomes more important as the propagation velocity of the reactive wave increases. Similar problems can also be encountered in process industries, involving hydrogen in the chemical process or as energy vector (natural gas reformers, fuel cells, etc.).

To deal with these safety issues empirical criteria have been developed in the early 2000s [1, 5] to discern possible FA or DDT scenarios. These criteria have proved to be powerful means in best estimate studies for the selection of the most relevant situations for which flame acceleration takes place. Moreover, thanks to the recent improvements in computer capabilities, numerical tools capable of simulating the propagation of a premixed hydrogen/air flame in large geometries were developed [2]. Still, the validation of these models remains of crucial importance to improve the safety of nuclear power plant. In the literature we can find a rich database on middle-scale experiments in confined geometries. Usually these experiments are performed in long tubes with uniformly distributed obstacles [6]. The majority of these devices are equipped with photodiodes, photomultiplier tubes or ionization probes allowing the detection of the combustion wave at different points along the tube axis. Despite their robustness, these techniques are able to capture only the monodimensional behavior of the flame front propagation. As a result, only a very coarse representation of the flame acceleration profile can be achieved.

The increasing demand for a deeper knowledge of flame acceleration mechanisms has pushed towards more accurate and sophisticated experimental techniques. An example of these improvements are visualization sections [7, 8]. Associated with Schlieren techniques and even with rapid field measurement techniques, such as Laser Doppler Velocimetry (LDV), Particle Image Velocimetry (PIV) or Planar Laser Induced Fluorescence (PLIF), they provide detailed and exhaustive data for the improvement and the validation process of numerical models. However, due to the brittleness of windows materials, most of the experiments were generally carried out with lean mixtures or at low initial pressure or even in open ended tubes. Unfortunately, these configuration are not representative of all the accident-related situations. The use of stainless steel tubes equipped with small instrumentation ports and narrow optical accesses remains therefore of great relevance in case of important overpressures. Thereby, the question of how to increase the measurement capabilities of these devices rises.

During the past year, a feasibility study was been performed at CEA Paris-Saclay laboratories to develop a technique capable to catch the flame position in a quasi-continuous way. SSEXHY (Structures Submitted to an EXplosion of HYdrogen) facility was used to this purpose. Previous attempts were made by Kuznetsov et alii [9] who used a single photodiode towards the tube axis to identify the transition time from deflagration to detonation. Oxygen light absorption measurement in detonation tubes, recently implemented by [10] to record variations in the equivalent ratio, constitutes a further example of time-resolved techniques.

In this work we developed a method for extrapolating the velocity profile by measuring the variation of the extension in depth of the fresh (or burnt) gas along the tube axis. It consists in performing IR-absorption measurements by doping the mixture with traces of alcanes such as methane. The advantages of using these compounds are first the small discrete region of absorption (C-H bond in "stretching mode" between 2850 and 2960 cm^{-1}) and second the fact that they do only exist in the unburnt gas. Special care was taken in correlating IR-absorption dependency on pressure and temperature variations. Correction factors were eventually obtained from the comparison between longitudinal (IR absorption measurements) and cross-sectional (photomultiplier tubes) flame velocity diagnosis techniques.

Finally, extensive comparisons among experimental results, numerical simulations and analytical models [3,

11] were drawn. From the literature [1] we know that, in an obstacle-laden tube, for a large spectrum of hydrogen concentrations, flame velocity increases rapidly up to a steady state value slightly lower than the Chapman-Jouguet deflagration velocity. Large-scale numerical simulations [2] give a good prediction of the asymptotic flame speed and pressure peaks; however the model fails in sizing up the outset of flame acceleration. For this reason, particular attention was payed to the early stages of the combustion, before compressible effects become preponderant.

2   Measurement techniques principles

Hydrogen/air mixture are unaffected by IR light; for this reason a small quantity of methane was added to the flammable mixture as tracer. The absorption in the infrared region of the C-H bond at 3.39 μm was then used to monitor the flame velocity. This absorption technique has been extensively employed to measure hydrocarbon concentration in situ [12]. It foresees the use of a laser beam that is attenuated by the gaseous mixture. The transmittance τ of the gaseous medium is given by the Beer-Lambert law:

$$\tau = \frac{I}{I_0} = \exp\left(-\frac{\sigma_i x_i P_0 l_t}{R T_0}\right) \tag{1}$$

with I the measured intensity, I_0 the light intensity throughout a non-absorbing medium, x_i the molar fraction of the absorbing chemical species, P_0 the total pressure, T_0 the temperature, l_t the length of the seeded zone, σ_i the absorption cross-section and R the perfect gas constant. If we suppose that only methane intervenes in absorbing IR light, $x_i \equiv x_{\mathrm{CH_4}}$ and $\sigma_i \equiv \sigma_{\mathrm{CH_4}}$.

Methane absorption-cross section was determined in our laboratory at ambient temperature and pressure by using the device shown in FIG. 1 (cf. [13]). The test cell features a stainless steel flanged tube with two sapphire windows at the extremities. The total length of the inner volume is 217 mm. The two windows allow the laser beam to pass through the test section. Helium-Neon Thorlabs H339P2 laser with 2 mW power was used to produce a beam at 3.39 μm. The laser beam is then chopped at 4000 Hz. Gaseous transmittance was recorded by a Thorlabs PDA20H PbSe detector placed at the end of the optical path. To reduce the influence of the environment surrounding the HeNe laser, a second detector (designated as reference detector in FIG. 1) is used in common-mode-rejection layout. Moreover, this technique allows more accurate measurements of I_0 (sapphire IR absorption is compensated by comparing light intensity at the two detectors).

Results are given in Table 1 and FIG. 2. They were found to be in accordance with the data existing in the literature [12, 14–17]. Dependence of $\sigma_{\mathrm{CH_4}}$ on the total pressure was derived as well, as shown in FIG. 2.

The uncertainty related to the measure of methane absorption cross section can be derived from equation (1):

$$\frac{u(\sigma_{\mathrm{CH_4}})}{\sigma_{\mathrm{CH_4}}} = \sqrt{\left(\frac{u(l)}{l}\right)^2 + \left(\frac{u(\chi_{\mathrm{CH_4}})}{\chi_{\mathrm{CH_4}}}\right)^2 + \left(\frac{u(P_0)}{P_0}\right)^2 + \left[\left(\frac{u(I)}{I}\right)^2 + \left(\frac{u(I_0)}{I_0}\right)^2\right]\left(\frac{1}{\ln\frac{I}{I_0}}\right)^2}. \tag{2}$$

Since all the measurements were performed at constant room temperature, the uncertainty related to the path length can be neglected (no dilatation effects). A value of 6% was obtained for the uncertainty of methane absorption cross section.
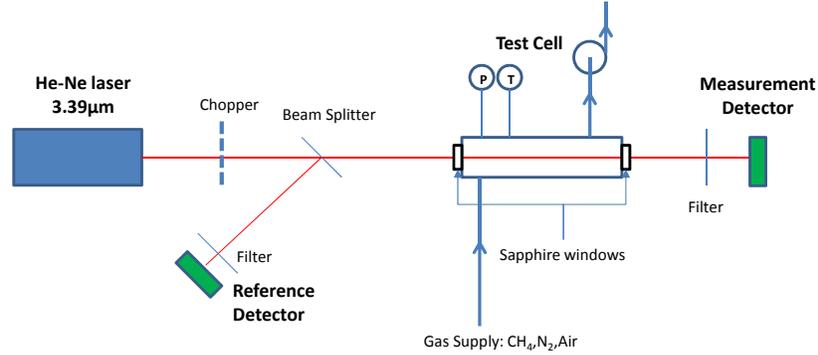
Figure 1: Test cell used to evaluate methane absorption cross-section.

Table 1: Comparison of methane absorption cross-section at 3.39μm at $P_0 = 1$ atm.

Reference	σ_{CH_4} [cm.atm]$^{-1}$	T_0 [K]
[14]	8.0	298
[15]	9.2	293
[16]	9.9	298
[12]	9.6	300
[17]	8.2	302
This work	8.2	298

2   Experimental apparatus

Flame acceleration experiments of premixed hydrogen/air mixture were carried out in the SSEXHY (Structures Submitted to a EXplosion of HYdrogen) combustion tube (FIG. 3). This tube is made of three sections with a total length of $l_t = 3930$ mm and an internal diameter of $D = 120$ mm. It is equipped with annular obstacles (blockage ratio BR $= 0.3$ or 0.6) located at one diameter distance along the path of the flame. The design pressure is 100 bar. Regarding the instrumentation, the tube is provided with 42 openings (40 lateral and two axial) to accommodate sensors. The dynamic pressure is measured using Kistler 601A, 6001 and 7001 piezoelectric pressure transducers, the shock wave in the unburnt gas is detected using Chimiemetal piezoelectric sensors, while the flame time-of-arrival is recorded using Hamamatsu R11568 photomultiplier (PM) tubes. PM tubes are coupled with an optical system designed to collect the light emitted by the OH$^\bullet$ radicals along the axis within very narrow solid angle. For the IR absorption measurement, two sapphire windows 5 mm thick were installed at both ends of the acceleration tube (FIG. 3). Laser optical scheme foresees the same elements described in FIG. 1. In addition, a second chopper was installed in front of the measurement detector to deal with flame light emission (as detailed in Chapter 3). The initial length of the absorption zone section is $l_t = L = 3930$ mm.

The flammable mixture is prepared by the method of partial pressures, starting by setting the tube under primary vacuum, then injecting methane (99.9995 % pure), hydrogen (99.9991 %) and, finally, air (20.9 % oxygen, 79.1 % nitrogen). A circulation pump is used for almost 30 minutes to homogenize the mixture inside the tube before ignition. At the end of the homogenization phase a gas sample is analyzed using a 490 micro-gas chromatograph (Agilent Technologies).
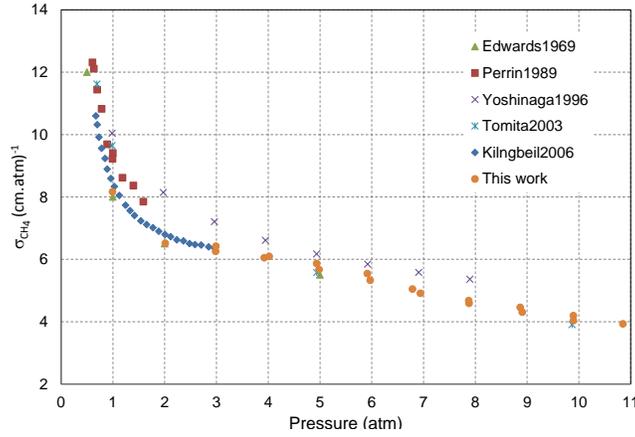
Figure 2: Effect of total pressure on methane absorption cross-section at 3.39μm.
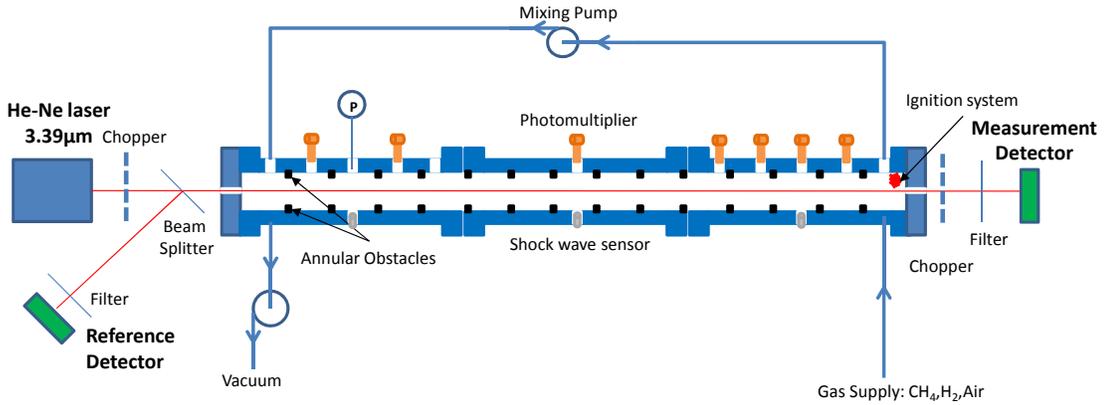

Figure 3: Schematic description of the SSEXHY facility.

In order to have access to the center line for IR measurements, the electrical spark used to ignite the mixture was moved upward (45 mm from the tube axis), on the gas injection line. Once ignited, the flame propagates along the obstacle-laden tube separating the fresh mixture from the burnt one. Since the quantity of methane is small compared to the other molecules, we can make the hypothesis that no methane remains in the burnt gas (complete combustion of methane). In this case, as methane is consumed by the flame, the absorbing path decreases and the transmittance across the tube increases.

By applying equation (1) to time-resolved IR absorption measurement, we obtain the variation of the depth of the fresh mixture in time, as:

$$l(t) = -\frac{RT(t)}{\sigma_{\mathrm{CH_4}}(P(t), T(t)) x_{\mathrm{CH_4}} P(t)} \ln \tau(t). \tag{3}$$

The flame tip propagation velocity is obtained deriving equation (3) in time:

$$V_{f,\mathrm{tip}} = \frac{\mathrm{d}x(t)}{\mathrm{d}t} = \frac{\mathrm{d}\left[l_t - l(t)\right]}{\mathrm{d}t}, \tag{4}$$

where $x(t)$ is the distance from the ignition point.

Since we are mostly interested in the early stages of flame propagation, when compressible effects as well as temperature changes in the fresh mixture can be neglected, we can simplify equation (3) assuming $P(t) = P(t_0) = P_0$ and $T(t) = T(t_0) = T_0$. This assumption is valid until either the ratio of burnt/fresh gas volumes exceeds few percents or a lead shock is formed ahead the reaction front. Beyond that, proper correction factors must be used to take into account pressure and temperature variations.

3   Experimental results and discussions

IR absorption technique was applied to different mixtures typical of lean hydrogen/air combustion: 23 and 15 vol% of hydrogen in dry air. The former flame is more stable than the latter one in terms of laminar flame stability analysis and, therefore, it presents less cellular structures in the flame front (see pictures of [18]).

Before performing the tests, several issues were investigated. First, the light emitted by the flame itself at 3.39μm was measured. The emission spectrum of hydrogen flames was recently published for a wide range of wavelengths in [19]. According to them, maximum flame irradiance occurs in the mid-infrared. At 3.39μm, flame irradiance is about one order of magnitude greater than the UV peak at 309 nm used for flame time-of-arrival measurements. In our experiences flame emission was measured by turning off HeNe laser and recording $I(t)$ with and without methane seeding. Results are shown in FIG. 4a and FIG. 4b. Here, an increase of intensity of the light emitted by the flame as it propagates along the tube was observed. To easily compare the two cases, the same scale for the ordinates was used to present the results. As expected, higher values were measured for the 23 vol% flame. Methane addition had a negligible effect.

The second important issue was the stability of the measured signal $I(t)$ in the presence of a propagating flame. For these tests, methane was not added and the laser was in operation. In the absence of any disturbing phenomena and besides flame light emission, the measured signal was expected to be constant and equal to that one measured in vacuum conditions (no absorbing species). Propagation of an unstable flame (15 vol%) leads to large oscillations of the recorded intensity as shown in FIG. 4c. Laser beam deflection by non normal density gradients in the flame front can be a possible explanation of this behavior. These oscillations were largely reduced by increasing the hydrogen content in the mixture (23 vol%) since the flame is less corrugated (see FIG. 4d). Consequently, we restricted our attention to the 23 vol% mixture. An important thing to stress out when interpreting Thorlabs PDA20H PbSe detectors output signal is that 0 V output signal corresponds to the time-averaged light intensity (for steady-state measurements). As the laser beam is chopped by a blade, the detector send a positive voltage output. On the other hand, when the sensitive area of the detector is enlightened, a negative voltage is provided. Light intensity is given by the amplitude of the oscillating wave response.

Water molecules at room temperature and pressure do not absorb light at 3.39μm. Nevertheless, as the temperature increases, mid-IR peaks become broader due to the Doppler effect. At the adiabatic flame temperature, mid-IR peaks overlaps the 3.39μm wavelength. By referring to HITRAN 2008 database [20], it was estimated that the absorption of 50 cm water column at adiabatic flame temperature and ambient pressure was less then 0.1%. Experimentally, water absorption was determined by subtracting the signal recorded during the "laser OFF" test case (flame emission) from that one recorded during the "laser ON" test case (laser transmission and flame emission), without methane seeding. The result, for the 23 vol% mixture, is shown in FIG. 5. As expected, the initial value (before the flame is formed) for the laser beam transmission was retrieved, proving that water vapor absorption at 3.39μm can be neglected.

(a) 15 vol% H2. Laser OFF: Flame emission.

(b) 23 vol% H2. Laser OFF: Flame emission.

(c) 15 vol% H2. Laser ON.

(d) 23 vol% H2. Laser ON.

(e) 15 vol% H2. $x - t$ diagram of flame propagation.
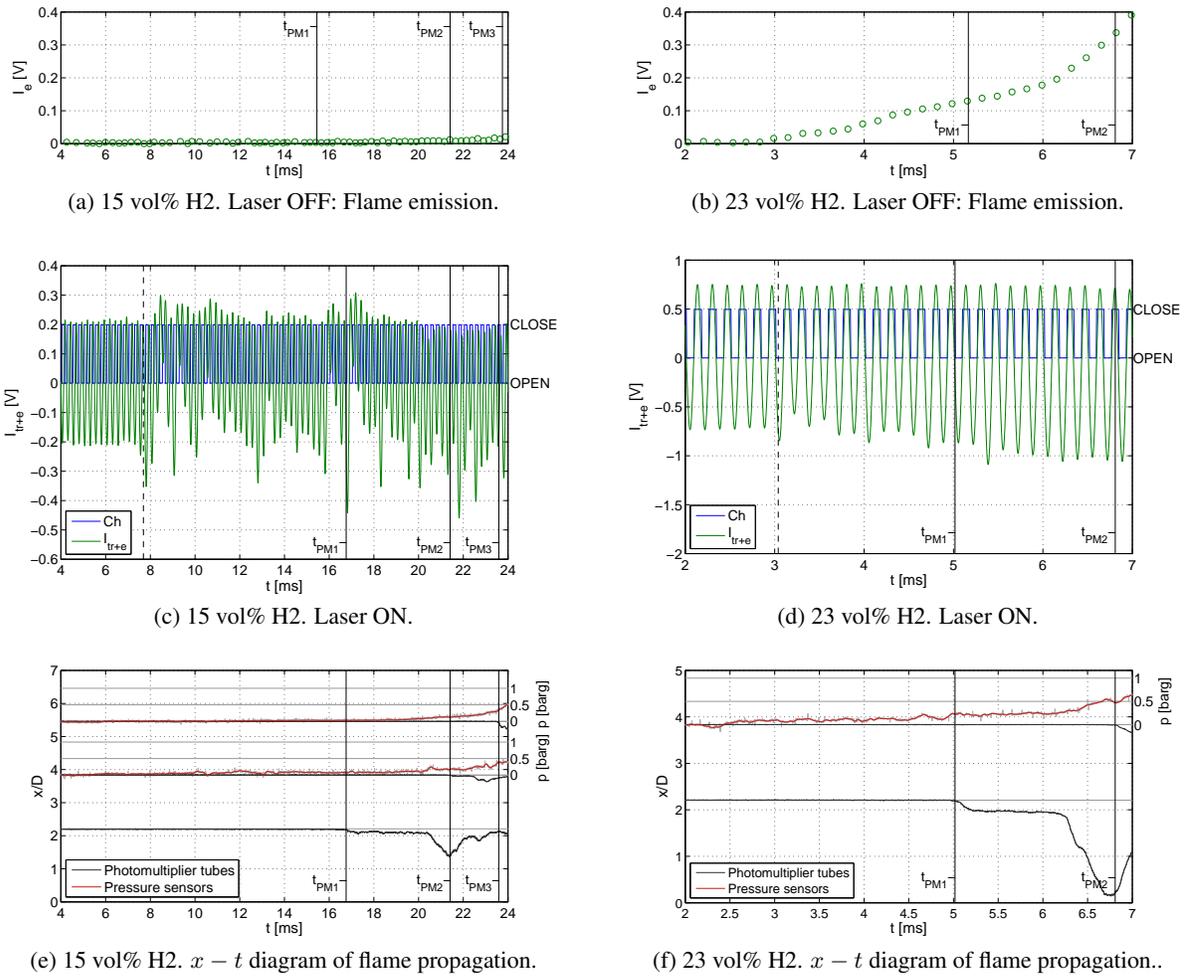
(f) 23 vol% H2. $x - t$ diagram of flame propagation..

Figure 4: Flame light emission and laser beam diffraction at 3.39μm for 15 and 23 vol% mixtures: Ch, chopper signal; I, light intensity measured by the detector; e, flame emission; tr+e, laser beam transmission + flame emission. Tests are synchronized on PM2 flame time-of-arrival.
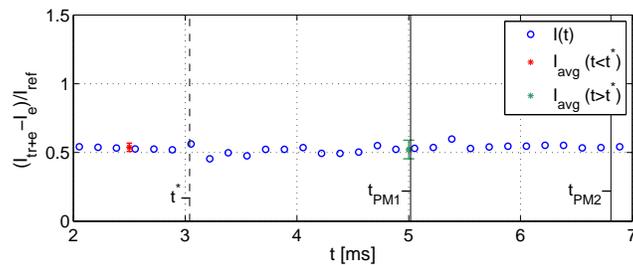

Figure 5: Laser beam transmission in time for the 23 vol% H2 mixture without methane. I, light intensity; e, flame emission; tr+e, laser beam transmission + flame emission; ref, reference detector; avg, time-averaged value.

Similarly, in case of methane addition, flame emission was subtracted from the total intensity, as shown in FIG. 6. By comparing the signal recorded by the measurement detector (red circles) and the ratio of this one and that one recorded by the reference detector (violet triangles), we may note the importance of the common-mode-rejection layout in dumping laser oscillations. Nevertheless, even if the light emitted by the flame was subtracted, the bias so introduced made difficult to use equation (3) to determine $l(t)$. A logarithmic fitting was then used to correlate $I(t)$ to $l(t)$. The perfect match between PM tubes signals and IR detector response was imposed to compute regression coefficients. The result, in terms of $x(t)$, is shown in FIG. 7.

Data so obtained are quite scattered. Moreover, for fast flames, as in this case, the frequency of the system chopper-detector is not high enough to allow measurements averaging. Thus, a regression function was used to fit the experimental data and derive the flame velocity profile. An exponential law (the solid blue line in FIG. 7) was chosen according to the analytical model presented in [21]. Due to the geometrical configuration described in the previous chapter, the flame originates 45 mm away from the tube axis. Then it is forced to move downward due to the presence of the first annular obstacle, located 3 mm away from the flange. The time t^* at which the flame intersects the laser beam is shown in FIG. 4c-d with a dashed black line. Most likely this intersection happens at $x > 0$. For this reason and in order to avoid the bias introduced by laser deflection while the flame crosses it, only those data in the range $3.5 < t < 7.5$ msec were considered for the fitting.

The exponential law matches well the behavior of the flame tip except in the region $t_{PM1} < t < t_{PM2}$. Repeating the experience the same trend was observed. As shown in the right hand of FIG. 7, this flame stagnation may be caused by the flame radial expansion inside the combustion chamber delimited by the third and the fourth obstacles. Further investigations are foreseen to clarify this point.
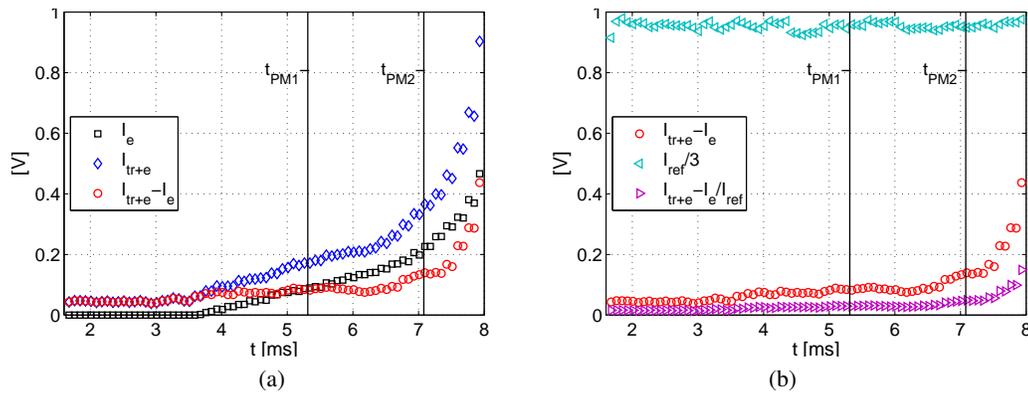

Figure 6: 23 vol% H2 with methane seeding. Signal processing. I, light intensity measured by the detector; e, flame emission; tr+e, laser beam transmission + flame emission; ref, reference detector.

The impact of methane addition on flame acceleration process was finally verified. As shown in FIG. 8b, the small quantity of methane added to the mixture had negligible effects on flame propagation.

The velocity profiles for both 15 vol% and 23 vol% mixtures are presented in FIG. 8. The main parameters of the combustion process are summarized in TAB. 2. Experimental results are given in terms of average values over three shots. Error bars identify maximum and minimum values of the shots. Flame acceleration profiles are consistent with those found in literature [22]. A chocked flame regime was reached at about 15
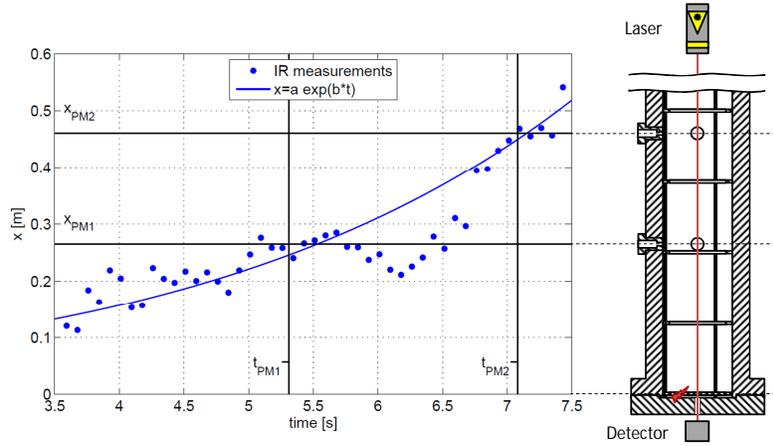
Figure 7: Flame tip propagation in time. $x_{\mathrm{PM}i}$ refers to the position of the i-th photomultiplier tube while $t_{\mathrm{PM}i}$ is the flame time-of-arrival measured by the i-th photomultiplier tube.

diameters from the ignition point for 15 vol% mixture. For 23 vol% mixture, the flame velocity reached a saturation value close to the CJ detonation velocity.

Table 2: Combustion parameters for hydrogen/air mixtures at room temperature and pressure.

Parameter	$\chi_{\mathrm{H}_2} = 15\%$	$\chi_{\mathrm{H}_2} = 23\%$
S_L [m/s]	0.24	1.11
σ	4.57	6.06
c_{su} [m/s]	374	391
c_{sb} [m/s]	767	914
V_{CJDF} [m/s]	720	897
V_{CJ} [m/s]	1524	1812
ν [m^2/s]	1.82×10^{-5}	1.98×10^{-5}

A zoom on the early stages of flame propagation for the 23 vol% mixture is shown in FIG. 9. Here, IR measurements are compared to those given by photomultiplier tubes. In addition, analytical expressions derived by Bychkov and colleagues [3, 11, 21] are also presented.

The acceleration of a premixed flame in a tube with repeated obstacles was theoretically described by [11,21] under the hypothesis of incompressible flow in the unburnt and burnt mixture. The velocity of the flame tip is given in the form:

$$V_f = \frac{4\,(\sigma - 1)\,S_L}{\sqrt{1 - \mathrm{BR}}} \left[1 + \frac{1}{2\,(\sigma - 1)} \right] \frac{x}{D} + \sigma S_L \tag{5}$$

with σ the expansion ratio, S_L the laminar flame velocity. This model (grey solid line in FIG. 9) only covers the initial phase of acceleration since the flame is assumed to be laminar, mono-dimensional in the tube and between the obstacles. Previously, Akkerman et al [23] proposed an analytical theory of flame acceleration in cylindrical smooth tubes in which the front accelerates exponentially according to the

(a) 15 vol% H2, BR= 0.3.
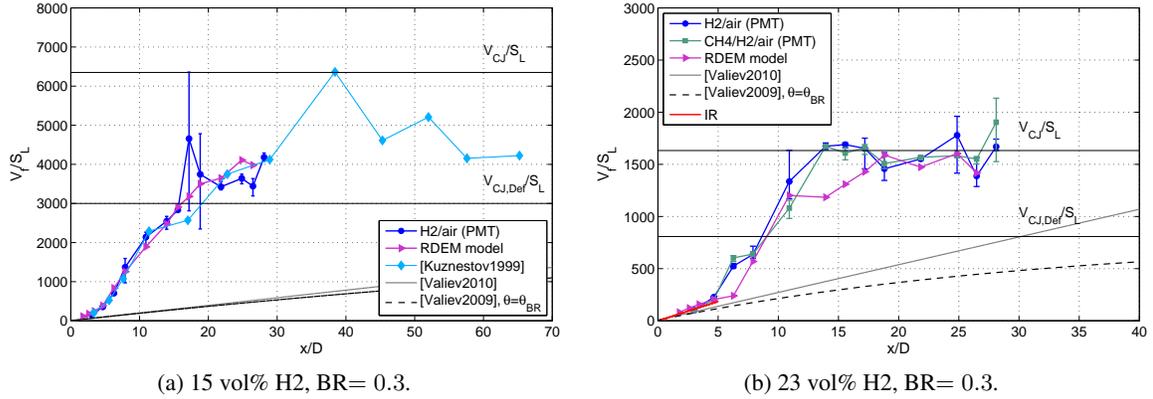

(b) 23 vol% H2, BR= 0.3.
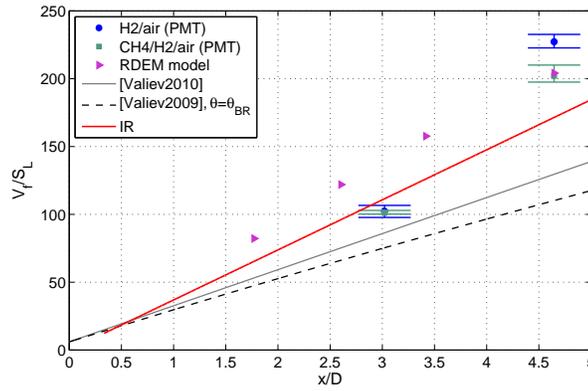
Figure 8: Velocity profile along the tube.

Figure 9: Zoom on the velocity profile along the tube for 23 vol% mixture.

following expression:

$$V_f = (\sigma - 1)S_L \exp\left(2\theta \frac{S_L t}{D}\right) \frac{I_0(\eta) - 1}{I_0(\eta) - 2\eta^{-1}I_1(\eta)} + S_L \tag{6}$$

where $\theta = \frac{Re}{4}\left(\left(1 + \frac{8(\sigma-1)}{Re}\right)^{\frac{1}{2}} - 1\right)^2$, $\eta = \sqrt{\theta Re}$ and I_i the modified Bessel function of order i. Recently, Valiev et al. [3] proposed to extend their first model empirically by adding a term in order to reach asymptotically a chocked velocity:

$$V_f = \sigma S_L \frac{\exp\left(2\theta \frac{S_L t}{D}\right)}{1 + \alpha \mathrm{Ma}\sigma \exp\left(2\theta \frac{S_L t}{D}\right)} \tag{7}$$

where $\mathrm{Ma} = \frac{S_L}{c_{su}}$ and $\alpha = \frac{S_L}{\mathrm{Ma} V_{\mathrm{CJDF}}}$.

By integrating equation (7) in time, it is possible to rewrite the expression of the velocity as a function of x/D. Dashed lines in FIG. 8 and FIG. 9 are obtained by substituting in equation (7) the acceleration rate for

smooth tubes, θ, with that one for obstacle-laden tubes, θ_{BR} [21]:

$$\theta_{\mathrm{BR}} = 2\frac{\sigma - 1}{\sqrt{1 - \mathrm{BR}}} \; . \tag{8}$$

Finally, a numerical model for flame acceleration dedicated to large geometries was developed [2, 24]. This simple model is based on the resolution of the Euler equations coupled to a diffuse interface propagation equation. Flame acceleration process is supplied by an algebraic equation for turbulent flame velocity. The application of this model to the present experiments is also given in FIG. 8 and FIG. 9 (violet line, RDEM model). Numerical results agree quite well with the experimental ones.

4 Conclusions

A method to measure the acceleration process of a premixed flame with a non intrusive technique was developed. It allows to track the flame front along the tube axis in a quasi-continuous way. The method demonstrated its capabilities in the early stages of flame propagation for a 23 vol% hydrogen in air mixture. For the moment, results must be interpreted in a qualitative way. For leaner mixtures, improvements are needed to reduce the effect of laser beam deflection by the flame. However, the deflection was small since the signal did not disappear completely. As a consequence, a finer laser beam combined with an optimized optical system could solve the problem. Moreover, laser-chopper-detector time response has to be increased to perform proper time resolved measurement. For rich flames, a seeding molecule in the oxidizer or the oxidizer itself will be more relevant. Oxygen absorption at 761 nm is currently under investigation.

References

[1] Dorofeev SB, Kuznetsov MS, Alekseev VI, Efimenko AA, Breitung W. (2001). Evaluation of limits for effective flame acceleration in hydrogen mixtures. Journal of Loss Prevention in the Process Industries. 14:583.

[2] Velikorodny A, Studer E, Kudriakov S, Beccantini A. (2015). Combustion modeling in large scale volumes using EUROPLEXUS code. Journal of Loss Prevention in the Process Industries. 35:104.

[3] Valiev D, Bychkov V, Akkerman V, Eriksson LE. (2009). Different stages of flame acceleration from slow burning to Chapman-Jouguet deflagration. Physical Review. 80:036317.

[4] The Steel Construction Institute. (2005). Protection of piping systems subject to fires and explosions. Health & Safety Executive.

[5] Breitung W, Chan C, Dorofeev SB, Eder A, Gelfand B, Heitsch M, Klein R, Malliakos A, Shepherd JE, Studer E, Thibault P. (2000). State-of-the-art report on flame acceleration and deflagration-to-detonation transition in nuclear safety. Technical report, Nuclear Energy Agency.

[6] Ciccarelli G, Fowler CJ, Bardon M. (2005). Effect of obstacle size and spacing on the initial stage of flame acceleration in a rough tube. Shock Waves. 14(3):161.

[7] Johansen CT, Ciccarelli G. (2009). Visualization of the unburned gas flow field ahead of an accelerating flame in a obstructed square channel. Combustion and Flame. 156:405.

[8] Boeck LR, Mével R, Fiala T, Hasslberger J, Sattelmayer T. (2016). High-speed OH-PLIF imaging of deflagration-to-detonation transition in H2air mixtures Exp Fluids. 57:105.

[9] Kuznetsov M, Ciccarelli G, Dorofeev SB, Alekseev V, Yankin Yu, Kim TH. (2002). DDT in methane-air mixtures. Shock waves. 12:215.

[10] Boulal S, Vidal P, Zitoun R. (2016). Experimental investigation of detonation quenching in non-uniform compositions. Combustion and Flame. 172:222.

[11] Bychkov V, Akkerman V, Valiev V, Law CK. (2010). Influence of gas compression on flame acceleration in channels with obstacles. Combustion and Flame. 157:2008.

[12] Tomita E, Kawahara N, Shigenaga M, Nishiyama A, Dibble RW. (2003). In situ measurement of hydrocarbon fuel concentration near a spark plug in an engine cylinder using the 3.392μm in frared laser absorption: discussions and applicability with a homogeneous methane-air mixture. Measurement science and technology. 14:1350.

[13] Mevel R, Boettcher PA, Shepherd JE. (2012). Absorption cross section at 3.39μm of alkanes, aromatics and substituted hydrocarbons. Chemical Physics Letters. 531:22.

[14] Edwards BN, Burch DE. (1965). Absorption of $3,39$-micron Helium-Neon laser emission by methane in the atmosphere. Journal of the Optical Society of America. 55(2):174.

[15] Perrin MY, Hartmann JM. (1989). High Temperature adsorption of the 3.39μm He-Ne laser line by methane. J. Quant. Spectrosc. Radiat. Transfer. 42(6):459.

[16] Yoshiyama S, Hamamoto Y, Tomita E, Minami KI. (1996). Measurement of hydrocarbon fuel concentration by means of infrared absorption technique with 3.39μm He-Ne laser. JSAE Review. 17:339.

[17] Klingbeil AE, Jeffries JB, Hanson RK. (2006).Temperature- and pressure-dependent absorption cross-sections of gaseous hydrocarbons at 3.39μ. Measuring Science and Technology. 17:1950.

[18] Goulier J, Comandini A, Halter F, Chaumeix N. (2017). Experimental study on turbulent expanding flames of lean hydrogen/air mixtures. Proceedings of the Combustion Institute. 36:2823.

[19] Arens EE, Youngquist RC, Starr SO. (2014). Intensity calibrated hydrogen flame spectrum. International Journal of Hydrogen Energy. 39:9545.

[20] Rothman LS, et al. (2009). The HITRAN 2008 molecularspectroscopicdatabase. JQSRT. 110:533.

[21] Valiev D, Bychkov V, Akkerman V, Law CK, Eriksson LE. (2010). Flame acceleration in channels with obstacles in the deflagration-to-detonation transition. Combustion and Flame. 157:1012.

[22] Kuznetsov M, Alekseev V, Bezmelnitsyn A, Breitung W, Dorofeev SB, Matsukov I, Veser A, Yankin Y. (1999). Effect of obstacle geometry on behavior of turbulent flames. Report IAE-6137/3 and FZKA-6328.

[23] Akkerman V, Bychkov V, Petchenko A, Eriksson LE. (2006). Accelerating flames in cylindrical tubes with nonslip at the walls. Combustion and Flame. 145:206.

[24] Beccantini A, Studer E. (2009). The reactive Riemann problem for thermally perfect gases at all combustion regimes. International Journal for Numerical Methods in Fluids. 76:662.